Nuclear Instruments and Methods in Physics Research A 1078 (2025) 170580

Contents lists available at ScienceDirect

Nuclear Inst. and Methods in Physics Research, A

journal homepage: www.elsevier.com/locate/nima

# Radiation hard multi-strip multi-gap resistive plate chamber architecture for low polar angles of the CBM-TOF wall

M. Petriş [a,*], V. Aprodu [a], I. Deppner [b], V. Duţă [a], J. Frühauf [b], N. Herrmann [c], M. Petrovici [a], A. Radu [a], E. Rubio [c]

[a] Hadron Physics Department, National Institute for Physics and Nuclear Engineering (IFIN-HH), Bucharest, Romania
[b] GSI Helmholtz Center for Heavy Ion Research GmbH (GSI), Darmstadt, Germany
[c] Physikalisches Institut der Universität Heidelberg, Heidelberg, Germany

## ARTICLE INFO

*Keywords:*
Gaseous detectors
Resistive plate chamber
Aging effect
Time resolution
Efficiency

## ABSTRACT

For the mitigation of the gas pollution effects in Multistrip Multigap Resistive Plate Chambers (MSMGRPCs) exposed to high irradiation doses, prototypes with a direct flow of the gas mixture through the gas gaps and discrete polyimide spacers were designed and assembled. The aging investigations of the chambers with the new design demonstrated negligible aging effects even for rather low gas flow rate. Two such prototypes were tested in real operation conditions, in an in-beam test performed at the SIS18 accelerator of GSI Darmstadt with reaction products. The obtained results are reported in this paper. They demonstrate the performance of the prototypes in terms of efficiency (>95%) and time resolution (~55 ps). Therefore, such direct flow MSMGRPCs will be implemented in the modular configuration of the low polar angle region of the CBM-TOF wall, called inner wall. Among the 12 modules of the CBM-TOF inner wall, the M0 module has the most complex structure. Details about the implementation of the direct flow MSMGRPCs of different granularities in the M0 module, whose assembling is in progress, are presented.

## 1. Introduction

The upgrade of the present running experiments as well as the construction of the next generation high energy physics experiments impose challenging performances to their experimental setups. The fix target Compressed Baryonic Matter (CBM) experiment [1] at the future Facility for Antiproton and Ion Research (FAIR) under construction in Darmstadt, aims to investigate very rare probes with high precision and enough statistics. For this reason, its experimental setup have to be able to cope with unprecedented high interaction rates of up to $10^7$ Hz. For the charged particle identification a Time of Flight (TOF) subsystem [2] based on multi-gap resistive plate chambers [3] with multi-strip readout [4] is included, its active area being defined by the acceptance of the silicon tracking system (polar angle between 2.5°–25°). Due to the high interaction rates at which the CBM experiment is designed to run, the chambers of the CBM-TOF wall have to cope with counting rates ranging between hundreds of Hz/cm$^2$ up to a few tens of kHz/cm$^2$, depending on their location [2,5].

The Multi-Gap, Multi-Strip, Resistive Plate Chamber (MSMGRPC) prototypes developed by our group are designed for the most demanding region of the CBM - TOF wall called inner wall, which covers polar angles between 2.5° and 12° [6]. The chambers of the CBM-TOF inner wall are required to keep an efficiency above 90% and a system time resolution better than 80 ps at foreseen counting rates from about 50 kHz/cm$^2$ at small polar angles (close to the beam pipe), towards 6 kHz/cm$^2$ at larger polar angles. In order to maintain their performance in high counting rate operation, the chambers will be equipped with low resistivity electrodes. The granularity requirements for different polar angle regions are fulfilled choosing different strip lengths, while the strip pitch is kept constant. Correspondingly, three types of chambers foreseen to be implemented in the CBM-TOF inner wall are defined [7], as it is detailed in Section 2.

MSMGRPC prototypes designed for the CBM-TOF inner wall were tested in high counting rate at the SIS18 accelerator of GSI Darmstadt. The measured efficiency was better than 95% at low counting rate and it has not deteriorated significantly (>90%) with the counting rate up to 30 kHz/cm$^2$ [8], the maximum available counting rate in the performed in-beam test. At the highest counting rate a 52 ps single chamber time resolution has been measured. The working gas mixture was flushed inside the housing box and the refreshment of the gas mixture in the gaps between the resistive electrodes was made in the classical way, through a diffusion process.

* Corresponding author.
*E-mail address:* mpetris@nipne.ro (M. Petriş).

https://doi.org/10.1016/j.nima.2025.170580
Received 12 December 2024; Received in revised form 23 April 2025; Accepted 24 April 2025
Available online 7 May 2025

A long term operation of a MSMGRPC in high counting rate could lead to aging effects. In order to investigate these effects, a chamber with gas exchange via diffusion was exposed to a 360 kCi $^{60}$Co source [9], available in IFIN-HH in Bucharest. A gas pollution effect was evidenced by the chemical composition of the layers deposited on the surfaces of the resistive electrodes as well as around the spacers of the tested prototype. The higher noise rates highlighted especially around the nylon spacers (fishing line) [10] could deteriorate the detector performance and artificial increase the data volume in a free-streaming data acquisition (DAQ) operation.

Our solution for minimization of such upshots has been the design of MSMGRPC prototypes with a direct flow of the gas mixture through the gaps between the resistive electrodes [8]. Flushing directly the active volume leads to a faster removal of the chemical pollutants that deposit around the spacers and on the surfaces of the resistive electrodes. Extensive aging tests of a direct flow MSMGRPC prototype performed using high X-ray fluxes demonstrated significant improvements brought by the new design. They were reflected in the reduced values of the dark currents and dark counting rates measured after irradiation in comparison with a prototype with gas exchange via diffusion [11]. Moreover, after the exposure to the high X-ray fluxes, very good performance in terms of efficiency (~95%) and time resolution (65 ps) were obtained in the laboratory measurements using cosmic rays [12]. Nevertheless, a mapping of the active area in a self-triggered mode operation of the DAQ system still revealed a noise rate located around the nylon spacer positions. For this reason we replaced the continuous nylon line by discrete polyimide pad spacers in order to minimize the active area in contact with the spacers and consequently reduce further the localized noise rate. The results obtained after the exposure of the direct flow prototypes with discrete spacers to a high X-ray flux demonstrated very low values of the dark current and dark counting rate, even at lower gas flow rate [12] in comparison with the ones used for prototypes assembled using nylon line spacers.

The work reported in this paper addresses the performance of the prototypes with a direct flow and polyimide discrete spacers in real operation conditions. It is further included the first steps to their implementation in the first CBM-TOF inner wall module, called M0. The constructive details of the prototypes, relevant for the reported work, are presented in Section 2. A more comprehensive description can be found in the Refs. [11,12]. The experimental configuration in the in-beam tests performed at the SIS18 accelerator of GSI Darmstadt together with the obtained results in terms of time resolution and efficiency are presented in Section 3. Details on the implementation of direct flow MSMGRPCs in the M0 module, whose configuration is the most complex among the twelve modules of the CBM-TOF inner wall, are presented in Section 4. Conclusions are presented in Section 5.

## 2. Constructive details of the direct flow MSMGRPC prototypes based on discrete spacers

The architecture of the direct flow prototypes (Fig. 1) is based on the typical configuration of the MSMGRPC prototypes with gas exchange via diffusion developed by our group [13,14]. A typical MSMGRPC chamber [15] has two stacks, each one of 5 gas gaps of 200 μm thickness, defined by 6 low resistivity glass electrodes (~$10^{10}$ Ω cm) [16] of 0.7 mm thickness. The strip readout anode is positioned in the middle, between the two stacks. It is sandwiched by the two positive high voltage electrodes isolated from the readout anode by two kapton sheets. The outermost electrodes of the prototype are the readout cathodes, also isolated from the negative high voltage electrodes by kapton sheets. The innovative strip structure for both readout and high voltage electrodes allows to tune the signal transmission line impedance [17] to match to the input impedance of the front-end electronics (FEE), avoiding the impact of signal reflexions on the experimental data in a free-streaming DAQ operation. The active area is defined by the 32 strips multiplied by the strip pitch (0.902 cm) and the strip length. As

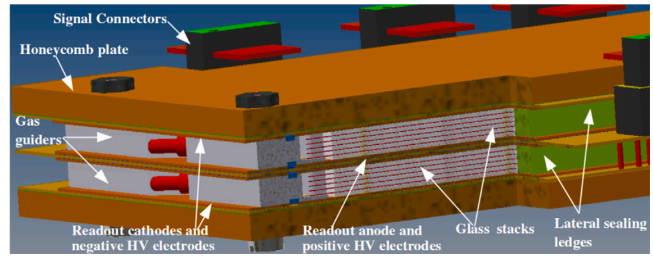


**Fig. 1.** Sketch of direct flow prototype configuration.

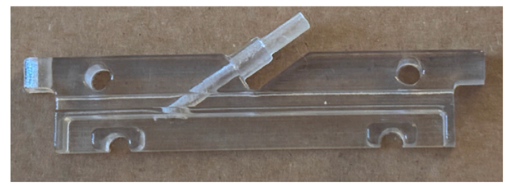

**Fig. 2.** Photo of a gas guide.

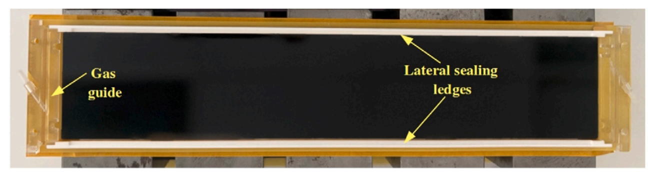


**Fig. 3.** The two ledges positioned parallel to the long sides of the glass plates and the two gas guiders installed at the two ends for gas inlet and outlet.

mentioned in Section 1, the CBM-TOF inner wall area is covered using three different granularity chambers (MRPC1a, MRPC1b, MRPC1c), differentiated only by their strip length (56 mm, 96 mm, 196 mm), while the strip pitch and inner geometry are identical. The 310 mm length of the glass plates is the same for all three types while their widths are of 60 mm for MRPC1a, 100 mm for MRPC1b and 200 mm for MRPC1c. The 310 mm is the current production limit of the size of the low resistivity glass, which also limits the length of the MSMGRPC chambers.

For the direct flow prototypes, the strips of both high voltage and read-out electrodes are centered relative to the glass edges and 4 mm shorter than the width of the resistive electrodes. This allows to position the two outermost spacer rows as much as possible outside of the action of the electric field, with the center of the spacer at 1.5 mm from the edge of the glass plate.

A gas guide provided with a tube for gas connection was designed and manufactured, as shown in Fig. 2. At the two ends of each glass stack (short side) were positioned two gas guiders, one for the injection of the gas flow through the gaps between the resistive electrodes and the other one for the exhaust (see Fig. 3). The gas volume of each of the two stacks of a MSMGRPC chamber is closed by two ledges positioned parallel to the long sides, the two gas guiders at the two ends for gas inlet and outlet (Fig. 3) and the two up and down high voltage (HV) electrodes. The gas volume was tightened on the outerside of the ledges by a thin silicon paste layer.

The first direct flow MSMGRPC prototype based on discrete spacers was assembled using 310 mm × 60 mm resistive electrodes and home made polyimide (kapton type) spacers of 200 μm thickness with a rectangular shape of 2 mm × 2 mm size. It will be called further P200. Searching on the market, we found commercially available polyimide spacers of 170 μm and a second prototype was assembled using them. It will be called further P170. The spacers were distributed with pitches of 30.7 mm along and of 28.5 mm across the length of the resistive electrodes [12].

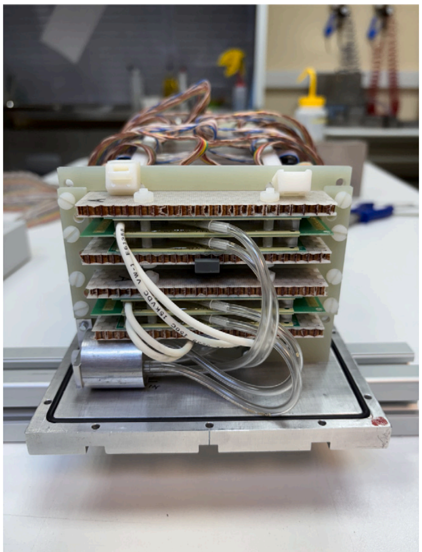

**Fig. 4.** The two prototypes assembled one on top of the other on the backpanel of housing box.

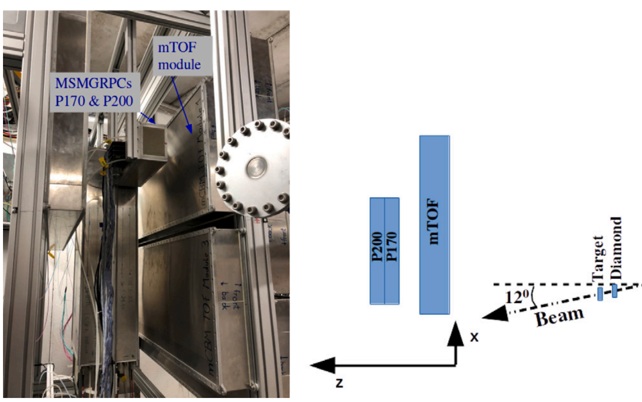


**Fig. 5.** Photo of the experimental setup (left). Sketch of the tracking setup (not at scale) (right).

Both of them have the highest granularity of the CBM - TOF wall corresponding to 56 mm strip length (MRPC1a). They were installed in the same housing box, P170 on top of P200 (Fig. 4). The signals are readout in a differential mode, both the positive and negative picked-up signals being fed into the input of a FEE readout channel. The aging investigations using a high X-ray flux, reported in a previous paper [12], demonstrated negligible aging effects even for a low gas flow rate of 8.4 ml/min. Taking into consideration these very positive results, a natural next step was to test the chamber's performances in - beam, in real operation conditions.

## 3. In-beam tests

### 3.1. Experimental setup

The two MSMGRPC prototypes based on discrete spacers (P200 and P170) were installed (see Fig. 5 - left side) in the mCBM experimental setup [18], currently in use at the SIS18 accelerator of GSI Darmstadt. The mCBM setup contains prototypes of all CBM subsystems, being a demonstrator of the CBM full data acquisition and analysis chains, as well as a setup for high counting rate tests.

Each chamber was flushed directly through the gas gaps with a gas mixture of 97.5%$C_2H_2F_4$ + 2.5%$SF_6$. The same gas mixture was also

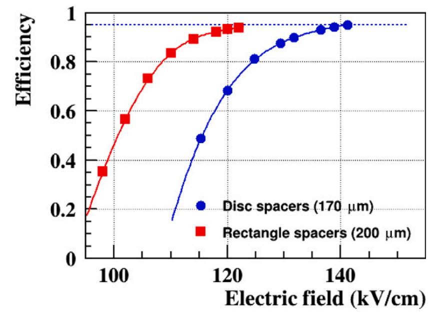


**Fig. 6.** Efficiency as a function of the electric field in the gas gap. The error bars are contained within the size of the symbols.

circulated through the housing box in order to maintain the gas quality in the chambers. The strips were readout at the both ends by front-end electronics motherboards designed for the inner wall [19]. Each motherboard contains 4 PADI XI amplifier-discriminator ASICs [20] and 8 self-triggered GET4 [21] time-to-digital converters. The digitized LVDS signals provide the time of arrival of the charged particle as well as the time-over-threshold (TOT) as measure for the input charge. The prototypes were positioned at an angle of 12 degrees relative to the beam axis. The tests were performed using reaction products of a $^{197}$Au beam of 1.2A GeV incident on a Au target.

For the measurement of the efficiency and time resolution a four station tracking setup (Fig. 5-right side) was defined (from upstream to downstream) by the beam reference detector (a strip diamond detector positioned in front of the target), a mTOF multi-gap resistive plate chamber with strip readout (270 mm × 300 mm active area, positioned inside the mTOF module) and the two P170 and P200 prototypes.

### 3.2. Results

The efficiency of each of the two prototypes was obtained using as reference tracks reconstructed in the three out of the four stations of the tracking setup and looking for a reconstructed hit in certain time and space windows in the fourth station, considered detector under test (DUT). The efficiency as a function of the electric field in the gas gap (Fig. 6) shows a plateau around 95% for both prototypes. As expected, for the thinner gap prototype P170, a higher field is needed in order to reach the same efficiency as with the P200 prototype. However, considering that the P200 prototype was the last one in the tracking setup, its efficiency measurement has been underestimated. Because it was not backed up by any other chamber, the reference tracks defined by the three stations in front of it could have tracks which already stopped in the P170 prototype. Therefore, the 95% efficiency measurement for P200 prototype is a conservative one. The measured time resolution was obtained as standard deviation of the Gauss function fitted to the distribution of the time difference between the measured and the expected time of arrival of particles in the chamber. The measured time was corrected for the rise time of the amplifying electronics (slewing corrections). The time spectra for the two prototypes are presented in Fig. 7 for applied high voltages corresponding to an electric field in the gas gap of 141 kV/cm for P170 and 122 kV/cm for P200, respectively. A chamber time resolution of 53 ± 2 ps was measured for P170 (see Fig. 7 left) and a 55 ± 2 ps for P200 (see Fig. 7 right). The value quoted here includes the intrinsic time resolution of the MSMGRPC prototype together with the contributions from electronics (amplification and time-to-digital conversion), uncertainties arising from the distribution of the digital clock in the experimental setup as well as contributions from the calibration and tracking.

Fig. 8 shows the measured values of the time resolution as a function of the electric field in the gas gap, showing slightly better values for the chamber with thinner gas gaps, as expected. The slight deterioration

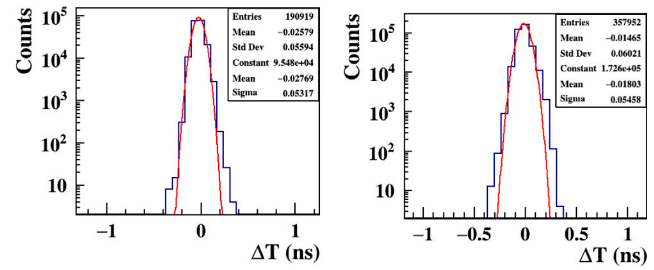


**Fig. 7.** Time difference distributions for P170 (left) and P200(right) for an electric field in the gas gap of 141 kV/cm (P170) and 122 kV/cm (P200).

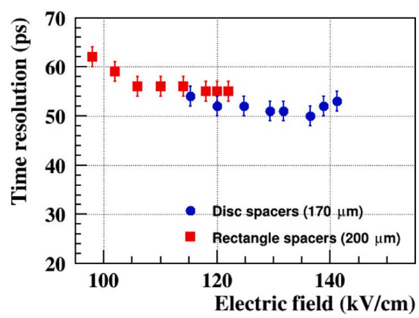


**Fig. 8.** Time resolution as a function of the electric field in the gas gap.

of the time resolution in the region of the efficiency plateau for P170 chamber could be due to the smaller avalanches which grow enough in the stronger electric field, such that the small induced signals cross the threshold with a larger spread of the temporal response, not fully corrected by the slewing corrections.

Taking into consideration the results of the in-beam test presented above and the good behavior of the direct flow prototypes with discrete spacers in the previously performed aging investigations, this type of chambers will be implemented in the inner zone of the CBM-TOF wall. In the assembling of the MSMGRPCs for the inner wall will be used spacers of 200 μm thickness which better fits with the gain of the PADI XI ASIC, enlarging the efficiency plateau. The implementation of the chambers in the inner zone of the CBM - TOF wall started with the assembling of the M0 module. This module is the most complex one, because it combines all three types of chambers of the inner zone, as it is shown in the next section.

## 4. Module M0

The modular design of the CBM-TOF inner wall [22] comprises 12 modules of 4 types (called M0, M1, M2 and M3), equipped with 316 MSMGRPCs of 3 types (see Section 2), all together counting 20224 readout channels. The design was optimized for a spatial overlap between the chambers inside each module, as well as between the modules, such to have a continuous coverage of the active area with a minimum number of chambers and readout channels. The M0 module will be equipped with 20 MRPC1a, 6 MRPC1b and 12 MRPC1c. The 2432 readout channels of M0 module amount to 12% from the total number of the readout channels of CBM-TOF inner wall. The sketch of the chamber positions across the backplane of the module is shown in Fig. 9. Inside the module, the chambers are distributed in z direction (along the beam pipe) on four levels with minimized overlaps of the neighboring chambers on $x$ (across the strips) and $y$ (along the strips) directions, in such a way that it is assured the detection of the incoming charged particles without dead zones. Two columns of MRPC1a chambers, with ten chambers per column are positioned at low polar angles, in the vicinity of the beam pipe. They are followed

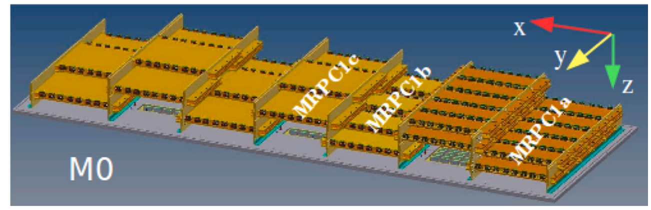


**Fig. 9.** Module M0 design.

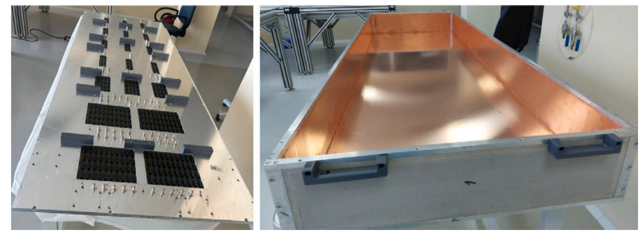

**Fig. 10.** The outer side of the backplane of the module M0 (left). Cover of the M0 module (right).

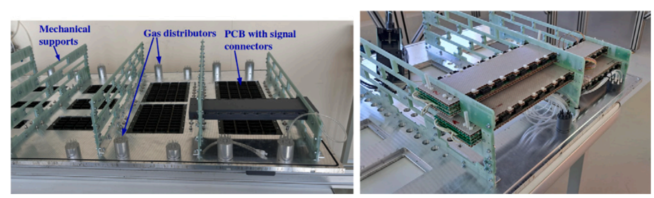


**Fig. 11.** Backplane equipped on the inner side with mechanical supports, FR4 plates with connectors, gas distributors (left). Chambers installed in the mechanical supports (right).

by a column of six MRPC1b chambers and four columns of MRPC1c chambers, with three chambers per column. The 38 MSMGRPCs are closed in a housing box which comprises a backplane (Fig. 10 - left) and a cover (Fig. 10 - right). The backplane of the module M0 was manufactured from an Al plate of 15 mm thickness. The outer side of the backplane is shown in Fig. 10 - left. All the feed-troughs for gas and high voltage connectors are worked out in the Al backplane. Printed circuit boards (PCB) with signal connectors soldered on both sides provides signal transmission from the chambers to the readout electronics (plugged - in on the outer side of the backplane). They are glued on rectangular holes machined in the Al backplane. On the inner side mechanical supports shown in Fig. 11 - left keep the chambers in precise positions which assure an uniform detection across the active area (Fig. 11 - right). Along the long edges of the module are mounted the gas distributors for both inlet and outlet of the gas mixture. They have cylindrical shape with 10 or 6 pipes of 4 mm diameter for gas distribution to/from the chamber's stacks and one 6 mm diameter central pipe for gas input/output. Their design assures an equal gas flow rate to each chamber. The ones with 10 output pipes (Fig. 12 - left) are designated to feed with gas the MRPC1a type chambers, while the ones with 6 pipes (Fig. 12 - right) are allocated to the MRPC1b and MRPC1c type chambers. For gas transport, pipes of the same length will be manufactured for each gas distributor, in such a way to assure the same gas flow rate to each chamber.

The module is closed by a cover made of a light composite material (10 mm honeycomb panel sandwiched between two 0.2 mm thin epoxy - glass fibers plates), electromagnetically shielded on the inner side by a thin copper foil (Fig. 10 - right). The joints of the housing box walls were tightened with araldite on the inner part and reinforced by aluminum L-profiles on the outer side.

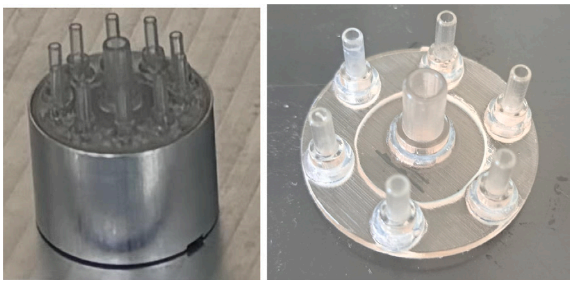

**Fig. 12.** The cylindrical gas distributor with ten pipes (left) and its top lead with six pipes (right) for output and a central pipe for input.

The components for the assembling of the MSMGRPC chambers, i.e. high voltage and readout electrodes, gas guiders, are already manufactured. They together with the low resistivity glass plates are already in house and the assembling of subcomponents as parts of a chamber is in progress. The disk shape spacers arrived recently in our laboratory, provided by Panel Group company from Taiwan [23]. This was the last missing items before running into the chamber assembling phase. A detailed report about the chamber assembling, installation in the M0 module and its tests will be a topic of a future paper.

## 5. Conclusions

The direct flow prototype based on discrete spacers are the solution for the mitigation of the aging effects observed in the MSMGRPCs exposed to high irradiation doses.

The in-beam tests of the direct flow prototypes showed the performance of this architecture in real experimental conditions. Taking into consideration the obtained results presented in this paper and the good behavior of the direct flow prototypes with discrete spacers in the aging investigations, this type of chambers will be implemented in the inner zone of the CBM-TOF wall.

The assembling of the first module (M0) of the CBM-TOF inner zone based on direct flow MSMGRPCs with discrete spacers is in progress.

## Declaration of competing interest

The authors declare that they have no known competing financial interests or personal relationships that could have appeared to influence the work reported in this paper.


## Acknowledgments

We would like to express our gratitude to all CBM colleagues involved in the mCBM activities, as well as to the SIS18/GSI accelerator crew.

This work was supported by Romanian Government Ministry of Research Innovation and Digitization, projects RO-FAIR 03/08.07.2024 and PN 23210103.


## References


[1] CBM Collaboration, Challenges in QCD matter physics - The scientific programme of the Compressed Baryonic Matter experiment at FAIR, Eur. Phys. J. A 53 (2017) 60, http://dx.doi.org/10.1140/epja/i2017-12248-y.

[2] CBM Collaboration, in: N. Herrmann (Ed.), CBM-TOF TDR, 2014, URL https://repository.gsi.de/record/109024.

[3] E. Cerron Zeballos, et al., A new type of resistive plate chamber: the Multigap RPC, Nucl. Instrum. Meth. A 374 (1996) 132, http://dx.doi.org/10.1016/0168-9002(96)00158-1.

[4] M. Petrovici, et al., Large - area glass-resistive plate chamber with multistrip readout, Nucl. Instrum. Meth. A 487 (2002) 337, http://dx.doi.org/10.1016/S0168-9002(01)02192-1.

[5] I. Deppner, et al., The CBM time-of-flight system, J. Instrum. 14 (2019) C09020, http://dx.doi.org/10.1088/1748-0221/14/09/C09020.

[6] I. Deppner, et al., The CBM time-of-flight wall - a conceptual design, J. Instrum. 9 (2014) C10014, http://dx.doi.org/10.1088/1748-0221/9/10/C10014.

[7] V. Duţă, et al., Update of the CBM-TOF Inner Wall Design, CBM Progress Report 2019, 2020, p. 134.

[8] M. Petris, et al., High time resolution, two-dimensional position sensitive MSMGRPC for high energy experiments, Nucl. Instrum. Meth. A 1045 (2023) 167621, http://dx.doi.org/10.1016/j.nima.2022.167621.

[9] IRASM center/IFIN-HH, Bucharest, URL https://www.nipne.ro/IRASM.php.

[10] D. Bartos, et al., Ageing studies of Multi-Strip Multi-Gap Resistive Plate Counters based on low resistivity glass electrodes in high irradiation dose, Nucl. Instrum. Meth. A 1024 (2022) 166122, http://dx.doi.org/10.1016/j.nima.2021.166122.

[11] V. Aprodu, et al., Aging suppression, high time resolution and 2D-position sensitive Multi-Strip Multi-Gap Resistive Plate Counter for high rate experiments, Nucl. Instrum. Meth. A 1049 (2023) 168098, http://dx.doi.org/10.1016/j.nima.2023.168098.

[12] M. Petris, et al., Aging suppression in Multistrip Multigap Resistive Plate Chambers for high counting rate experiments, Nucl. Instrum. Meth. A 1066 (2024) 169584, http://dx.doi.org/10.1016/j.nima.2024.169584.

[13] M. Petrovici, et al., High counting rate, two dimensional position sensitive timing RPC, J. Instrum. 7 (2012) P11003, http://dx.doi.org/10.1088/1748-0221/7/11/P11003.

[14] M. Petris, et al., Performance of a two-dimensional position sensitive MRPC prototype with adjustable transmission line impedance, Nucl. Instrum. Meth. A 920 (2019) 100, http://dx.doi.org/10.1016/j.nima.2018.12.074.

[15] M. Petriş, et al., Performance of the MSMGRPC with the highest granularity of the CBM-TOF wall in cosmic ray tests, Romanian J. Phys. 66 (2021) 305.

[16] J. Wang, et al., Development of high-rate MRPCs for high resolution time-of-flight systems, Nucl. Instrum. Meth. A 713 (2013) 40, http://dx.doi.org/10.1016/j.nima.2013.02.036.

[17] D. Bartos, et al., A method to adjust the impedance of the transmission line in a multi-strip multi-gap resistive plate counter, Romanian J. Phys. 63 (2018) 901.

[18] CBM Collaboration, mCBM@SIS18, 2019, http://dx.doi.org/10.15120/GSI-2019-00977.

[19] J. Frühauf, et al., Hardware Development for CBM ToF, CBM Progress Report 2012, 2013, p. 67.

[20] M. Ciobanu, et al., PADI, an Ultrafast Preamplifier - Discriminator ASIC for Time-of-Flight Measurements, IEEE Trans. Nucl. Sci. 61 (2014) 1015, http://dx.doi.org/10.1109/TNS.2014.2305999.

[21] H. Deppe, H. Fleming, The GSI event - driven TDC with 4 channels GET4, IEEE Nucl. Sci. Symp. Conf. Rec. (2009) 295, http://dx.doi.org/10.1109/NSSMIC.2009.5401741.

[22] M. Petris, et al., Towards the construction of the inner zone of the CBM-TOF wall, J. Phys.: Conf. Ser. 1555 (2020) 012014, http://dx.doi.org/10.1088/1742-6596/1555/1/012014.

[23] Panel Group, URL https://panel.com.tw.